

Accommodation of Curtailed Wind Power by Electric Boilers Equipped in Different Locations of Heat-supply Network for Power System with CHPs

Yunfeng Ma, Yang Yu, and Zengqiang Mi

Abstract—Electric boilers (EBs) provide an alternative method to deal with the accommodation of curtailed wind power. To pursue the minimum coal consumption in the system, a dispatching model integrating combined-heat-and-power (CHP) plants and EBs in different locations is developed, and the penalty of wind power curtailment and cost of EB employment are also incorporated in the model. The transmission loss and transportation lag of heat-supply network as well as the elasticity of heat load are considered in this paper. A kind of constrained programming with stochastic and fuzzy parameters is applied to deal with the uncertainties. A case in East Inner Mongolia in China demonstrates that the EBs are able to absorb curtailed wind power and supply the heat. The results indicate that the utility of EBs in the primary or secondary heat-supply network to accommodate curtailed wind power is mainly related to the efficiency of heat transmission and the elasticity of heat load.

Index Terms—Wind power, combined-heat-and-power (CHP) unit, electric boiler (EB), heat-supply network.

I. INTRODUCTION

IN recent years, the installed capacity of wind power in China increased rapidly, with an average annual growth of 25.7% from 2010 to 2018. By the end of 2018, the total installed capacity of wind power reached 184.26 GW [1]. We explore a representative area, East Inner Mongolia (EIM) in China, where the curtailed wind power reached more than 7.2 billion kWh in 2018. This area underwent a rapid expansion of wind power from 1.66 GW in 2005 to 28.69 GW in 2018, and has been planned to reach 45.00 GW in 2020 [2]. The power produced in EIM power grid

primarily satisfies local power load. Only about 15% of wind power is exported to the external larger power grid. Restricted by small local demand and rapid increase of wind power, the proportion of curtailed wind power increased from almost zero in 2005 to 25% in 2016.

Based on coordinated operation of thermal system and power system, wind power consumption is promoted and can adapt to the difference between the peak load and valley load. In the literature, there are lots of research works, which review the operation and applications of energy storage technologies [3]-[6], as well as their potential costs [7]. Considering the combination of heat and electricity, the technologies include combined-heat-and-power (CHP) plants, heat pumps [8]-[12], heat storage and electric boilers (EBs) [13], [14].

In a power system with CHP units, the allocation of electric heat pumps or EBs could relax the heat-electric constraints of CHP units and allow more wind power integrated into the power grid. A few studies have demonstrated the superiorities of EB in increasing wind power penetration in different countries [15]-[21]. Reference [17] analyzes the employment of EB for heating in China, and the results suggest that the deployments of EBs may provide a more cost-effective way than pumped hydro storage facilities to reduce wind power curtailment.

Previous studies indicate that the curtailed wind power declines with the enlargement of EBs for heating. The flexible start-up and convenient installation endow EBs with a natural feature to adapt to the fluctuation of heat load. Reference [18] uses a central EB to integrate with a stand-alone wind power. Reference [20] supplies an auxiliary thermal source using heat storage and EB to decouple the heat and power. Reference [21] designs a joint scheduling scheme of power and heat to curtail wind power through installing EBs in the secondary heat-supply network.

The above studies mainly concentrate on discussing the effectiveness of EBs in consuming high penetration of wind power. However, the equipped location of EBs has been hardly investigated, which is important because the equipped location of EBs would influence the accommodation of wind power directly or indirectly when the heat network character-

Manuscript received: November 9, 2019; accepted: June 1, 2020. Date of CrossCheck: June 1, 2020. Date of online publication: July 30, 2021.

This work was supported by the Fundamental Research Funds for the Central Universities (No. 2020MS095), the Headquarter of Science and Technology Project for State Grid Corporation of China (No. KJGW2018-014), and National Key R&D Program of China (No. 2018YFE0122200).

This article is distributed under the terms of the Creative Commons Attribution 4.0 International License (<http://creativecommons.org/licenses/by/4.0/>).

Y. Ma and Z. Mi are with the School of Electrical and Electronic Engineering, North China Electric Power University, Beijing, China (e-mail: hdmymf0928@163.com; mizengqiang@sina.com).

Y. Yu (corresponding author) is with the Department of Electrical Engineering, North China Electric Power University, Baoding, China (e-mail: ncepu_yy@163.com).

DOI: 10.35833/MPCE.2019.000151



istics are considered. Reference [22] demonstrates that the transportation lag and transmission loss of the primary heating network may have an impact on the wind power accommodation in the integrated power and heat energy systems. In [23], a detailed district heating network (DHN) model is established to analyze its energy storage capability for managing the variability of wind energy. However, the dispatching model does not conclude EBs and the DHN model is sophisticated to some extent. References [24] and [25] have established the dispatching model of CHP system considering the characteristics of heat network and thermal comfort. However, further sensitivity studies on how these factors impact the accommodation results are not performed and the location of EBs in the district heat network is not discussed.

Hence, we develop an alternative scheme by introducing EBs into EIM power grid to reduce curtailed wind power and discuss how the different locations of EBs in heat-supply network influence the utility to accommodate curtailed wind power.

In comparison with the current research works, the main contributions of this paper can be summarized as follows.

1) A novel scheme of installing EBs in secondary heat-supply network (SHSN) or in primary heat-supply network (PHSN) is proposed to integrate with high penetration of wind power. Four different schemes considering no EBs, EBs only in PHSN, EBs only in SHSN, and EBs both in PHSN and in SHSN are designed to accommodate curtailed wind power in power systems containing a coal-fired CHP.

2) Considering the transmission loss and transportation lag of heat-supply network, the uncertainties of wind power and power load, and elasticity of heat load, an economic dispatching model combining power load, heat load, and wind power is constructed to achieve the aim of least coal consumption for the developed four schemes.

3) To deal with the uncertainties, the existing literature mostly regards the wind power generation or power load as single random variables or single fuzzy variables. Considering different characteristics of wind power and power load, a kind of constrained programming with stochastic and fuzzy parameters is applied.

The rest of this paper is organized as follows. Section II analyzes the mechanism of accommodating curtailed wind power in a power system with CHPs. Section III designs the scheme for accommodating curtailed wind power through equipping EBs in different locations of heat-supply network. The dispatching model aiming at obtaining minimum coal consumption is constructed in Section IV. A case in EIM power grid is analyzed in Section V, and the conclusion is drawn in Section VI.

II. MECHANISM ANALYSIS FOR ACCOMMODATING CURTAILED WIND POWER

A. Relation of Heat-power Coupling in CHP and Thermal Power (TP) Plants

The relation of heat-power coupling in CHP plants impacts on the accommodation of wind power in power grid directly. Considering the commonly used air-extraction CHP plant, its operation characteristic between heat and power is

shown in [26]. Under the condition of pure condensing, the maximum and minimum power outputs of the turbine are $P_{e,max}$ and $P_{e,min}$, respectively. With the increasing extraction of the steam, the power reduces proportionally. When the thermal power (TP) is P_h , the regulation interval of power for the plant ranges only from $P_{e,h,min}$ to $P_{e,h,max}$, which indicates a relatively limited ability to accommodate wind power. As shown in Fig. 1, for a pure condensing TP plant, its minimum output has a reasonable lower bound, which is a constant.

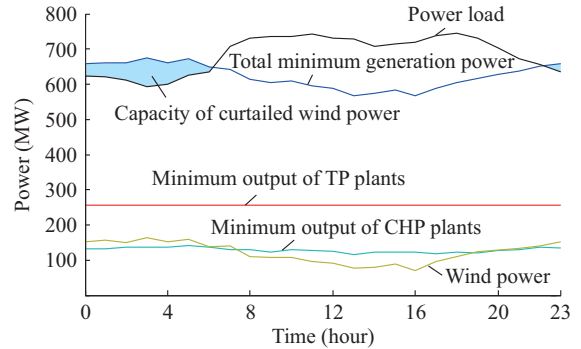


Fig. 1. Load and generation curves of various units.

B. Accommodating Curtailed Wind Power Using EBs

At night, the power load of EIM power grid is very low, but the output of wind power is usually the largest in the day. Additionally, the increasing heat load in winter raises the forced output of CHP plants. Hence, combining the two types of plants leads to a lot of redundant power. To maintain the security and stability of power grid, some TP plants may need to be shut down. Once the generated power is higher than the power load of the power grid, wind power has to be curtailed to avoid the shut down of some TP plants, as shown in Fig. 1. The load and generation curves of various units in power system including EBs are shown in Fig. 2. During the period of wind power curtailment, EBs are used for peak-shaving start-up and undertake a part of heat load. The forced output of CHPs declines with the reduction of heat load. The power load of the power grid increases concurrently with the absorption of electric energy by EBs. Therefore, the goal of accommodating curtailed wind power is achieved.

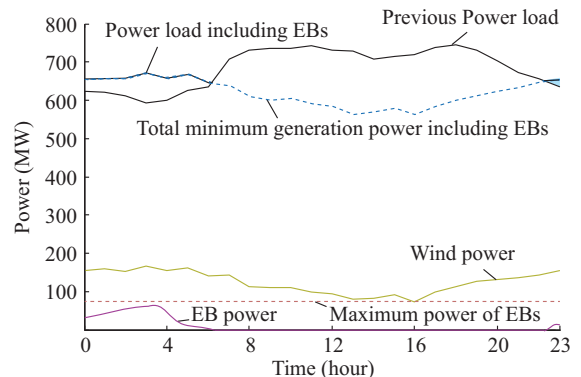


Fig. 2. Load and generation curves of various units in power system including EBs.

III. ACCOMMODATION SCHEME OF WIND POWER CURTAILMENT BY EBS

For wind power curtailment, the configuration of EBs in the heat-supply network can decouple the heat-power coupling for CHP plants and enhance the ability to accommodate wind power. For the installation location of the EBs, we design a scheme of the EBs installed at the supply side or load side to accommodate wind power, which is shown in Fig. 3. The specific configuration of the EBs in PHSN or SHSN is described in Fig. 4. According to the configuration of the EBs in the system, there are four schemes: no EBs, EBs only in PHSN, the EBs only in SHSN, and EBs both in PHSN and SHSN. The allocation of EBs at the supply side or PHSN could play an important role [16]. However, the accommodation of wind power curtailment will be reduced considering the heat loss between PHSN and SHSN, which can be attributed to the restriction of heat-power coupling of CHP plant. If the EBs are deployed at the load side and work together with the CHP units, its ability to accommodate wind power curtailment may be expanded.

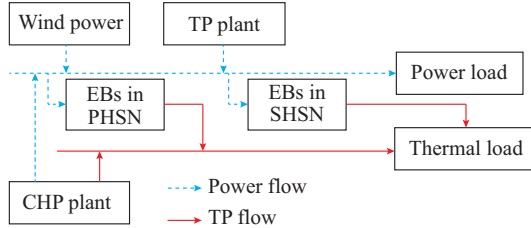


Fig. 3. Schematic diagram of EBs deployed to accommodate wind power curtailment.

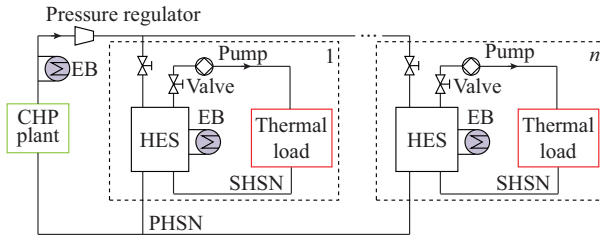


Fig. 4. Specific diagram of EBs configured in PHSN and SHSN.

The purpose of the proposed scheme is to increase the EBs in PHSN or in SHSN for peak-shaving, and the effectiveness of the four schemes will be evaluated. The main heat sources are CHP plants, which are responsible for basic heat load. As another kind of heat sources, the EBs offer the regulation of peak load in the heating system. Owing to the lower power load, higher heat load, and larger output of wind power at night in winter, wind power curtailment occurs more frequently. Hence, heat load provided by CHP plants can be reduced at night with the increasing power load consumed by the EBs, which may free up more space for higher penetration of wind power. Furthermore, the proposed scheme also has the following advantages.

1) The EBs are able to satisfy the fluctuant heat load rapidly and precisely with the merits of fast start-up feature.

2) Practically, the residential heat network is naturally composed of several SHSNs. The capacity of each EB allocated in these SHSNs is relatively small, and the scheme in-

cluding multiple EBs in SHSNs is more practical than that including single EB with a huge capacity.

3) The objective of EBs working together in PHSN and SHSN is similar to accomplish coarse and fine adjustments of the heat load. EBs dispersedly installed in some heat exchange stations (HESs) of SHSN are close to the center of heat load, which are able to accurately adjust the heat load with lower thermal losses. Whereas EBs deployed in PHSN can coordinately work with CHP plants and achieve the adjustment of the heat load in the whole heat network.

IV. DISPATCHING MODEL FOR OPTIMAL ACCOMMODATION OF WIND POWER CURTAILMENT BY EBS

A. Power System Modeling

The power system contains three primary kinds of power plants including TP plants, CHP plants and wind power plants. The simple structure of the 3-node power grid is shown in Fig. 5.

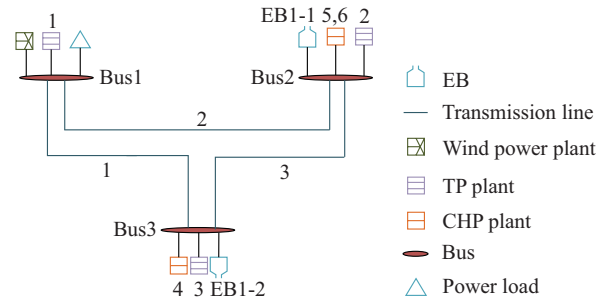


Fig. 5. Simplified structure of power grid.

1) TP and CHP Plants

$$F_{TP} = a_{1i} (P_{TP}^{c,t})^2 + a_{2i} P_{TP}^{c,t} + a_{3i} \quad (1)$$

$$F_{CHP} = b_{1i} + b_{2i} P_{CHP}^{d,t} + b_{3i} D_{CHP}^{d,t} + b_{4i} (P_{CHP}^{d,t})^2 + b_{5i} P_{CHP}^{d,t} D_{CHP}^{d,t} + b_{6i} (D_{CHP}^{d,t})^2 \quad (2)$$

where F_{TP} is the coal consumption of TP unit; a_{1i} , a_{2i} , and a_{3i} are the parameters indicating coal consumption; F_{CHP} is the coal consumption of CHP unit; b_{1i} , b_{2i} , b_{3i} , b_{4i} , b_{5i} , and b_{6i} are the parameters describing coal consumption; $P_{TP}^{c,t}$ and $P_{CHP}^{d,t}$ are the generated power at time t for the c^{th} TP and the d^{th} CHP units, respectively; and $D_{CHP}^{d,t}$ is the quantity of stream extraction at time t for the d^{th} CHP unit.

The output of TP plants must be bounded between the maximum and minimum power values.

$$P_{TP,\min}^{c,t} \leq P_{TP}^{c,t} \leq P_{TP,\max}^{c,t} \quad c \in \{1, 2, \dots, z_1\}, t \in \{1, 2, \dots, T\} \quad (3)$$

where $P_{TP,\min}^{c,t}$ and $P_{TP,\max}^{c,t}$ are the minimum and maximum power at time t for the c^{th} TP plant, respectively; z_1 is the number of TP units; and T is the number of scheduling periods.

Additionally, the rates of ramp-up and ramp-down for TP plants within a certain time interval should be controlled in a reasonable range.

$$r_{TP}^{c,t,\text{down}} \Delta t \leq P_{TP}^{c,t} - P_{TP}^{c,t-1} \leq r_{TP}^{c,t,\text{up}} \Delta t \quad c \in \{1, 2, \dots, z_1\}, t \in \{1, 2, \dots, T\} \quad (4)$$

where $r_{TP}^{c,t,\text{down}}$ and $r_{TP}^{c,t,\text{up}}$ are the rates of ramp-up and ramp-

down at time t for the c^{th} TP plant; and $\Delta t = 1$ hour is the dispatching interval time.

During the start-up process, the power output of TP plant satisfies the following condition:

$$\begin{cases} s_{TP}^{c,t-1} = 0 \\ s_{TP}^{c,t} = 1 \\ s_{TP}^{c,t+1} = 0 \\ P_{TP}^{c,t} = P_{TP,\min}^{c,t} \end{cases} \quad (5)$$

where $s_{TP}^{c,t}$ describes the running status for the c^{th} TP unit, and 0 denotes the shut-down process and 1 denotes the start-up process.

The outputs of power and TP are within the ranges of the minimum value and the maximum value, respectively.

$$P_{CHP,\min}^{d,t} \leq P_{CHP}^{d,t} \leq P_{CHP,\max}^{d,t} \quad d \in \{1, 2, \dots, z_2\}, t \in \{1, 2, \dots, T\} \quad (6)$$

$$D_{CHP,\min}^{d,t} \leq D_{CHP}^{d,t} \leq D_{CHP,\max}^{d,t} \quad d \in \{1, 2, \dots, z_2\}, t \in \{1, 2, \dots, T\} \quad (7)$$

$$P_{CHP}^{d,t} = k_d D_{CHP}^{d,t} \quad d \in \{1, 2, \dots, z_2\}, t \in \{1, 2, \dots, T\} \quad (8)$$

where $P_{CHP,\min}^{d,t}$ and $P_{CHP,\max}^{d,t}$ are the minimum and the maximum power at time t for the d^{th} CHP unit, respectively; $D_{CHP,\min}^{d,t}$ and $D_{CHP,\max}^{d,t}$ are the minimum and the maximum quantities of stream extraction at time t for the d^{th} CHP unit, respectively; z_2 is the number of CHP units; and k_d is the coefficient depicting the relation between power and the quantity of extraction stream.

Similarly, the rates of ramp-up and ramp-down for CHP plant should also be restricted.

$$r_{CHP}^{d,t,\text{down}} \Delta t \leq P_{CHP}^{d,t} - P_{CHP}^{d,t-1} \leq r_{CHP}^{d,t,\text{up}} \Delta t \quad d \in \{1, 2, \dots, z_2\}, t \in \{1, 2, \dots, T\} \quad (9)$$

where $r_{CHP}^{d,t,\text{down}}$ and $r_{CHP}^{d,t,\text{up}}$ are the rates of ramp-up and ramp-down at time t for the d^{th} CHP unit, respectively.

2) Constraints of Power Network

For each bus v at time t , the power consumed by power load and EBs is balanced with the sum of the power transmitted from other buses, and the power generated by TP plants, CHP plants and wind farms.

$$P_{TP}^{i,L,v} + P_{CHP}^{i,L,v} + P_W^{i,L,v} + \sum_{k=1}^n P_{TL,k}^{i,L,v} = P_L^{i,L,v} + P_{EB}^{i,L,v} \quad (10)$$

where $P_W^{i,L,v}$ is the consumed wind power; $P_L^{i,L,v}$ is the power load at time t ; n is the number of the transmission lines at bus v ; and $P_{TL,k}^{i,L,v}$ is the power transmitted by transmission lines connected to bus v .

Meanwhile, the transmission power on each transmission line should be limited by:

$$\left| P_{TL,k}^{i,L,v} \right| \leq P_{TL,k,\max}^{i,L,v} \quad (11)$$

where $P_{TL,k,\max}^{i,L,v}$ is the transmission limit of the transmission line k . A linear DC power flow model [27] is applied to calculate the power flow.

3) Constraint of Wind Power

The predicted wind power should be equal to the sum of the curtailed wind power and the consumed wind power.

$$P_W^i + P_{CW}^i = P_{WP}^i \quad t \in \{1, 2, \dots, T\} \quad (12)$$

where P_{WP}^i is the predicted power of wind power at time t ; and P_{CW}^i is the curtailed wind power at time t .

4) Constraints of EBs

The consumed power for EBs should be lower than the

maximum value of power.

$$0 \leq P_{EB1}^{m,t} \leq P_{EB1,\max}^m \quad m \in \{1, 2, \dots, z_3\}, t \in \{1, 2, \dots, T\} \quad (13)$$

$$0 \leq P_{EB2}^{n,t} \leq P_{EB2,\max}^n \quad n \in \{1, 2, \dots, z_4\}, t \in \{1, 2, \dots, T\} \quad (14)$$

where $P_{EB1,\max}^m$ and $P_{EB2,\max}^n$ are the maximum power for the m^{th} EB in PHSN and the n^{th} EB in SHSN, respectively; and z_3 and z_4 are the total numbers of EBs in PHSN and SHSN, respectively.

5) Chance constraints Considering Uncertainties of Wind Power and Power Load

The constraint of the power indicated in (10) disregards the uncertainties of wind power generation and power load. If the prediction values of wind power generation and power load are regarded as definite values, the uncertainties of wind power generation and power load can be embodied by their prediction errors. Then, the condition of equality constraint for bus 1 can be updated and rewritten as below through the introduction of related chance constraints.

$$Pos \left\{ \Pr \left\{ P_{TP}^{i,t} + \sum_{k=1}^n P_{TL,k}^{i,L,v} + P_W^i + \tilde{e}_W^i = P_L^i + \zeta_L^i \geq \alpha_1 \right\} \geq \alpha_2 \right\} \quad (15)$$

where \tilde{e}_W^i is the prediction error of wind power at time t ; ζ_L^i is the prediction error of power load at time t ; α_1 is the confidence level of random variable ζ_L^i ; α_2 is the predetermined confidence level of fuzzy variable \tilde{e}_W^i ; and $Pos\{\cdot\}$ denotes the possibility of the event in $\{\cdot\}$.

Influenced by various environmental factors such as air temperature and humidity, the output error of wind power is frequently difficult to be expressed by statistical property. Hence, the prediction error of wind power is given as a fuzzy variable, which is more consistent with its characteristic. In practice, the prediction error \tilde{e}_W^i is represented as a triangular fuzzy variable and its triangular fuzzy parameter and membership function $\mu(\cdot)$ can be expressed as:

$$\tilde{e}_W^i = (-v_W^i, 0, v_W^i) \quad (16)$$

$$\mu(e_W^i) = \begin{cases} v_W^i - e_W^i & 0 < e_W^i < v_W^i \\ \frac{e_W^i + v_W^i}{v_W^i} & -v_W^i < e_W^i < 0 \\ 0 & \text{else} \end{cases} \quad (17)$$

where v_W^i is the threshold value of the prediction error.

Furthermore, one of the features for the power load is the periodicity to some extent. The prediction error of the power load is insensitive to the prediction time and is proportional to the size of power load. Therefore, the prediction error is represented as a Gaussian statistical variable, which is given as:

$$\zeta_L^i: N\left(0, (\sigma_L^i)^2\right) \quad (18)$$

$$\sigma_L^i = \frac{P_L^i}{100} \quad (19)$$

where $(\sigma_L^i)^2$ is the variance.

For the fuzzy case, we use the fuzzy simulation method [28] to handle the possibility constraint $Pos\{\cdot\} \geq \alpha_2$.

B. Heat System Modeling

1) Heat Source

The heat production of a CHP plant $Q_{CHP}^{i,L,j}$ can be calculat-

ed as:

$$Q_{CHP}^{i_1,t,j} = D_{CHP}^{i_1,t,j} \frac{\Delta H_{CHP}^{i_1,t,j}}{1000} \quad (20)$$

$i_1 \in \{1, 2, \dots, l_1\}, t \in \{1, 2, \dots, T\}, j \in \{1, 2, \dots, A\}$

where $D_{CHP}^{i_1,t,j}$ is the quantity of stream extraction at time t in the j^{th} heat-supply area for the i_1^{th} CHP unit; and $\Delta H_{CHP}^{i_1,t,j}$ is the enthalpy drop of stream extraction at time t in the j^{th} heat-supply area for the i_1^{th} CHP unit.

$$Q_{EB1}^{m,t} = 3.6\eta_1^m P_{EB1}^{m,t} \quad m \in \{1, 2, \dots, z_3\}, t \in \{1, 2, \dots, T\} \quad (21)$$

$$Q_{EB2}^{n,t} = 3.6\eta_2^n P_{EB2}^{n,t} \quad n \in \{1, 2, \dots, z_4\}, t \in \{1, 2, \dots, T\} \quad (22)$$

where $Q_{EB1}^{m,t}$ and $Q_{EB2}^{n,t}$ are the heat production of the m^{th} EB in PHSN and the n^{th} EB in SHSN at time t , respectively; and η_1^m and η_2^n are the conversion efficiencies from electricity to heat for the m^{th} EBs in PHSN and the n^{th} EBs in SHSN. Equations (21) and (22) imply that the heat of the EBs should also meet certain constraints limited by (13) and (14).

2) HES

HESs are modeled as the isolation device between the PHSN and SHSN. The heat loss in HES is neglected and the transmission loss of primary heat-supply network is considered.

3) Heat Network

The heat network has been simplified to the line networks, where all consumers receive hot water from a single supply pipe and direct the cooled water to a single return pipe as shown in Fig. 5. Reference [29] shows that when using the proper simplification method, the calculation error would not significantly increase.

Since the scale of SHSN is smaller than that of PHSN, we mainly consider the characteristics of PHSN in two aspects: the transportation lag and transmission loss. Δt is the time required for the water moving from the producer to the consumers [30]. The total lag in a network can be characterized by the time required for the water travelling from the producer to the farthest consumer and back at some nominal flow velocity. The transportation lag in the water pipeline of length L is:

$$\Delta t = \frac{L\pi r^2 \rho}{4G_t} \quad (23)$$

where r is the hydraulic radius; ρ is the density of the fluid; and G_t is the mass flow rate.

The transmission loss in the water pipeline of length L is:

$$\Delta Q = \frac{L(T_i - T_0)}{\sum_{i=1}^n \frac{1}{2\pi\lambda_i} \ln \frac{d_i}{d_{i-1}}} \quad (24)$$

where d_i is the outside diameter of the i^{th} layer of insulation material; T_i is the temperature of the water in the pipeline; T_0 is the temperature on the surface of the pipe; n is the number of layers of the material; and λ_i is the thermal conductivity.

4) Elasticity of Heat Load

When the heating temperature changes within a certain range, it will not affect the user comfort. In this paper, we provide more space for wind power accommodation by utilizing the elasticity of demand for the heat load.

$$\begin{cases} Q_{j,\min}^t (1 - k_{down}) Q_j^t \\ Q_{j,\max}^t = (1 + k_{up}) Q_j^t \end{cases} \quad (25)$$

where $Q_{j,\min}^t$ and $Q_{j,\max}^t$ are the minimum and maximum heat loads that satisfy the user comfort, respectively; and k_{down} and k_{up} are the coefficients of the elasticity of the heat load.

5) Constraint of Heat Load

For a PHSN, the heat exchange power of HES is equal to the heat production of CHP plants and EBs minus the transmission loss. Considering the characteristics of PHSN, the relation is given as:

$$\sum_{i_1=1}^{l_1} Q_{CHP}^{i_1,t,j} + \sum_{i_2=1}^{l_2} Q_{EB1}^{i_2,t,j} - k_q \Delta Q = \sum_{i_3=1}^{l_3} Q_{HES,1}^{i_3,t+\Delta t,j} \quad (26)$$

$t \in \{1, 2, \dots, T\}, j \in \{1, 2, \dots, A\}$

where l_1 , l_2 , and l_3 are the numbers of CHP units, EBs in PHSN, and EBs in SHSN, respectively; k_q is the coefficient of the transmission loss, which varies between 0 and 1; A is the number of heat supply area; $Q_{CHP}^{i_1,t,j}$ is the heat production of the i_1^{th} CHP by the i_1^{th} CHP units at time t in the j^{th} heat-supply area; and $Q_{HES,1}^{i_3,t+\Delta t,j}$ is the heat power absorbed by the i_3^{th} HES at time t in the j^{th} heat-supply area.

For an SHSN, the heat load is balanced with heat production of HES and EBs in SHSN, which is described as:

$$\sum_{i_3=1}^{l_3} Q_{HES,2}^{i_3,t,j} = Q_j^t - \sum_{i_3=1}^{l_3} Q_{EB2}^{i_3,t,j} \quad t \in \{1, 2, \dots, T\}, j \in \{1, 2, \dots, A\} \quad (27)$$

$$\sum_{i_3=1}^{l_3} Q_{HES,1}^{i_3,t,j} = \sum_{i_3=1}^{l_3} Q_{HES,2}^{i_3,t,j} \quad (28)$$

$$Q_{j,\min}^t \leq Q_j^t \leq Q_{j,\max}^t \quad (29)$$

where Q_j^t is the heat load at time t in the j^{th} heat-supply area; and $Q_{HES,2}^{i_3,t,j}$ is the heat production released by the i_3^{th} HES at time t in the j^{th} heat-supply area.

C. Dispatching Model

This subsection establishes an economic dispatching model for wind power accommodation by EBs, which aims to pursue the minimum coal consumption considering multi-energy and the loss of heat-supply network.

1) Objective Function

CHP plants undertake the heating task and cannot be started up or shut down arbitrarily. Compared with CHP plants, the start-up costs for EBs and wind farm are relatively low. Hence, the costs of which are disregarded. The objective function in economic accommodation of curtailed wind power is constructed as:

$$\min \sum_{t=1}^T \sum_{c=1}^{z_1} (F_{TP} (P_{TP}^{c,t}) + \varphi_{TP}^{c,t} s_{TP}^{c,t} (1 - s_{TP}^{c,t-1})) + \sum_{d=1}^{z_2} F_{CHP} (P_{CHP}^{d,t}, D_{CHP}^{d,t}) + \varepsilon P_{CW}^t + \chi_1 \sum_{m=1}^{z_3} P_{EB1}^{m,t} + \chi_2 \sum_{n=1}^{z_4} P_{EB2}^{n,t} \quad (30)$$

where z_1 , z_2 , z_3 , and z_4 are the numbers of TP units, CHP units, EBs in PHSN, and EBs in SHSN, respectively; $\varphi_{TP}^{c,t}$ is the start-up cost at time t for the c^{th} TP unit; P_{CW}^t is the curtailed wind power at time t ; ε is the penalty coefficient; $P_{EB1}^{m,t}$ and $P_{EB2}^{n,t}$ are the dispatched power at time t for the m^{th} EBs and the n^{th} EBs in PHSN and SHSN, respectively; and χ_1

and χ_2 are the cost coefficients.

2) *Constraints*

1) Constraints of power balance: the generation and demand of electricity are balanced during each period. The constraints of the power balance are defined as related chance constraints in (15)-(19).

2) Constraints of the heat balance are defined in (26)-(28) and can be rewritten as:

$$Q_{j,\min}^{t+\Delta t} \leq \sum_{i_1=1}^{I_1} Q_{CHP}^{i_1,t,j} + \sum_{i_2=1}^{I_2} Q_{EB1}^{i_2,t,j} - k_q \Delta Q + \sum_{i_3=1}^{I_3} Q_{EB2}^{i_3,t+\Delta t,j} \leq Q_{j,\max}^{t+\Delta t} \quad (31)$$

- 3) Constraints of TP plants are defined in (3)-(5).
- 4) Constraints of CHP plants are defined in (6)-(9).
- 5) Constraints of transmission lines are defined in (11).
- 6) Constraints of EBs are defined in (13), (14), (21) and (22).
- 7) Constraints of wind power are defined in (12).

V. CASE STUDY

A. *Data Sources and Experiment Design*

The experiment data are originated from the EIM power grid in China, which includes three TP plants (TP1, TP2, TP3), three CHP plants (CHP4, CHP5, CHP6), and a wind farm with 150 MW rated power. The parameters of TP and CHP plants are shown in Tables I and II, respectively. The location of EBs equipped in PHSN can be seen from Fig. 5 and the EBs in SHSNS is equipped at five HESs. The capacities of the EBs at different locations are given in Table III, which are about 20% of the heat load. The sampling frequency of the data is one hour, and the sampling data are utilized for day-ahead dispatching, which is shown in Fig. 6.

TABLE I
PARAMETERS OF TP PLANTS

Unit	Capacity (MW)	a_{1i}	a_{2i}	a_{3i}
TP1	300	21.2678	0.1715	0.000189
TP2	100	23.8905	0.2716	0.000261
TP3	100	23.8945	0.2809	0.000237

TABLE II
PARAMETERS OF CHP PLANTS

Unit	Capacity (MW)	b_{1i}	b_{2i}	b_{3i}	b_{4i}	b_{5i}	b_{6i}
CHP4	300	2.005	0.434	0.123	0.0009	0.00019	0.00021
CHP5	150	2.236	0.401	0.128	0.0008	0.00018	0.00026
CHP6	150	2.226	0.412	0.126	0.0007	0.00017	0.00025

TABLE III
CAPACITIES OF EBs EQUIPPED WITH DIFFERENT SCHEMES

Scheme	Capacity (MW)						
	EB1-1	EB2-1	EB2-2	EB1-2	EB2-3	EB2-4	EB2-5
Scheme 2	15			20			
Scheme 3		7.0	8.0		3.60	5.80	10.60
Scheme 4	3	5.6	6.4	4	2.88	4.64	8.48

The case is simulated through four schemes as follows.

- 1) Scheme 1: there are no EBs in the heat-supply network.
- 2) Scheme 2: there are EBs only in PHSN.

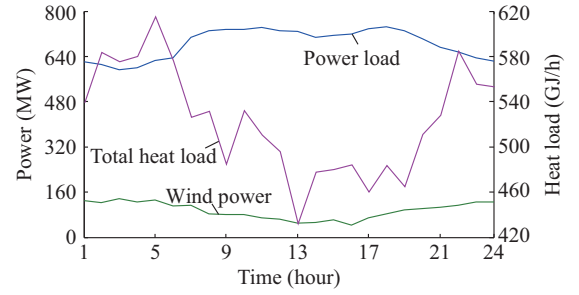


Fig. 6. Original data of heat load, power load, and wind power.

- 3) Scheme 3: there are EBs only in SHSNs.
- 4) Scheme 4: there are EBs both in PHSN and in SHSNs.

The first scheme implies that the heat load is satisfied only by CHPs. In this situation, the coupling between the heat and power is rigid, which leads to curtailed wind power. The last three schemes increase EBs to supply heat and accommodate the curtailed wind power coordinated with CHPs. EBs are installed at different locations in every scheme. Due to the heat transportation lag of the primary heat network, the heat load is meant to be moved in the time scale, which may lead to different utilities of the EBs to accommodate the wind power. Besides, we discuss how the heat transmission loss affects the accommodation results by introducing the coefficient k_q .

B. *Results and Discussion*

1) *Effect of EBs to Accommodate Curtailed Wind Power*

Coal consumptions with different losses of heat-supply network in the four schemes are compared in Fig. 7 when both the elasticity coefficients of the heat load are 0.15. It indicates that, except scheme 1, the other three schemes have basically the same coal consumption of 8220 kg/kWh with zero loss of heat-supply network. With the increasing loss, the coal consumptions in four schemes all increase.

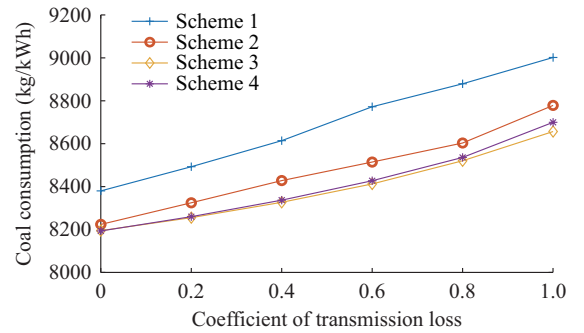


Fig. 7. Comparison of coal consumptions in four schemes.

The optimized results at different confidence levels are compared in Table IV without heat supply loss in scheme 1. Random confidence level α_1 reflects the implementation opportunity of stochastic wind power. For a larger value of α_1 , Table IV presents that there is a high probability that the combined output of wind power and TP plants is larger than the power load. Fuzzy confidence level α_2 reflects the achieved possibility of fuzzy variable under uncertain condition, which embodies the estimation of the scheduling personnel to the prediction value of wind power. A larger value

of α_2 indicates a higher accuracy of wind power prediction, which requires low regulation of TP plants and results in a low running cost.

TABLE IV
OPTIMIZED RESULTS OF COAL CONSUMPTION AT DIFFERENT CONFIDENCE LEVELS

α_1	α_2	Coal consumption (kg/kWh)
0.60	0.80	8419
0.80	0.60	8659
0.80	0.80	8543
0.80	0.95	8499
0.95	0.80	8792

Figure 8 presents the curtailed wind power curve with different heat loss coefficients in four schemes. In scheme 1, when the heat loss coefficient changes, the curtailed wind power always occurs between 1:00 a.m. and 7:00 a.m. Besides, curtailed wind power increases with the efficiency reduction of heat-supply network. This is because CHP units need to generate more heat to compensate the heat loss, which leads to more redundant power. When the EBs are connected to the system, curtailed wind power in scheme 2, 3 and 4 decreases compared with that of scheme 1. It is actually the EBs that accommodate the curtailed wind power. When the heat transmission efficiency is 100%, the wind power under the three schemes can be completely absorbed. Merely, the curtailed wind power enlarges with the efficiency reduction.

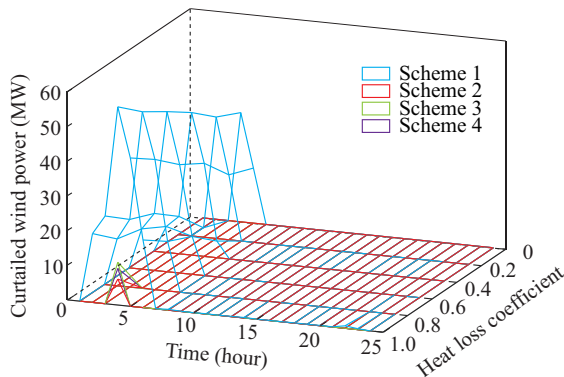


Fig. 8. Curtailed wind power curve with different heat loss coefficients.

In the four schemes, the total outputs of TP plants, CHP plants and wind farm are shown in Fig. 9(a)-(c), respectively. For TP plants shown in Fig. 9(a), the total output basically trends with the power load. Furthermore, the total output of TP plants in scheme 1 is the lowest in the four schemes during the whole dispatching time. In scheme 1, the heat load is only balanced by CHP units, which leads to a large output of power due to the rigid coupling relation of heat and power in CHP units. On the other hand, coal consumption in wind power is smaller than that in TP plants. To achieve the minimum coal consumption, wind power will be preferentially utilized to undertake the power load. The remaining portion of power load is satisfied by TP plants. Therefore, the output of TP plants declines naturally. For

CHP plants shown in Fig. 9(b), a similar trend with the variation of heat load exists in their total power outputs. In the three schemes with EBs connected, the total power outputs become smaller compared with those of scheme 1, especially within the time of wind power curtailment from 23:00 p.m. to 5:00 a.m. with the highest heat load in the system. Combined with Fig. 9(c), it demonstrates that the curtailed wind power is practically absorbed by EBs and is converted into the heat consumed by heat load.

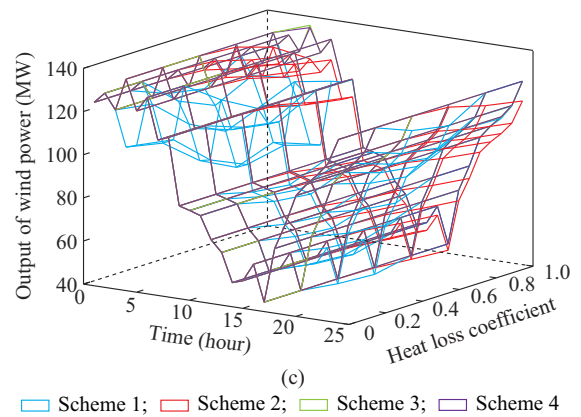
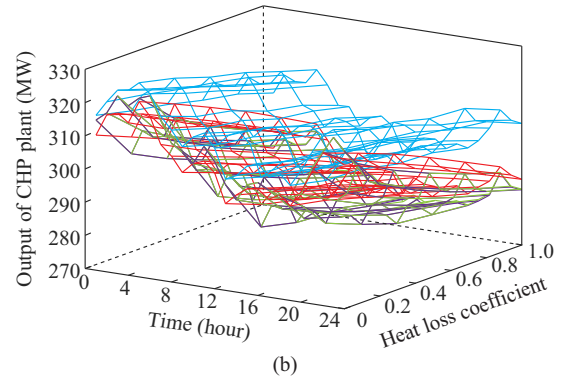
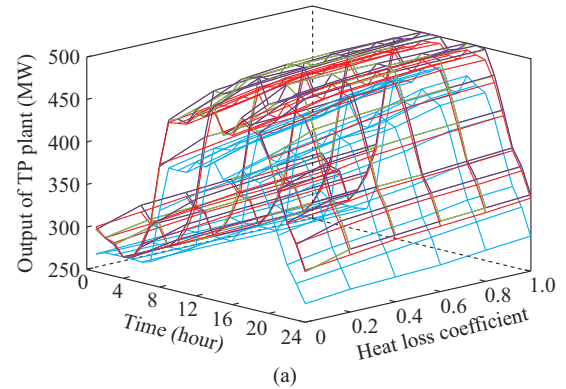


Fig. 9. Comparison of outputs of TP plant, CHP plant and wind power in four schemes. (a) Output of TP plant. (b) Output of CHP plant. (c) Output of wind power.

2) Difference Between EBs in PHSN and SHSN

To further analyze the differences between the two schemes where the EBs are equipped at different locations, two more sets of cases considering different elasticity coefficients of heat load and transmission loss are simulated. The results are shown in Fig. 10(a) and (b), respectively. Figure 10(a) takes both the elasticity coefficients of heat load as ze-

ro and Fig. 10(b) takes both the elasticity coefficients of heat load as 0.25. It indicates that with the decrease of elasticity coefficient and heat loss coefficient, the advantages of scheme 2 become more and more prominent. In other words, with the increase of elasticity coefficient and heat loss coefficient, the most operation cost will be saved by scheme 3 among the four schemes. And scheme 4 is always in the middle of schemes 2 and 3.

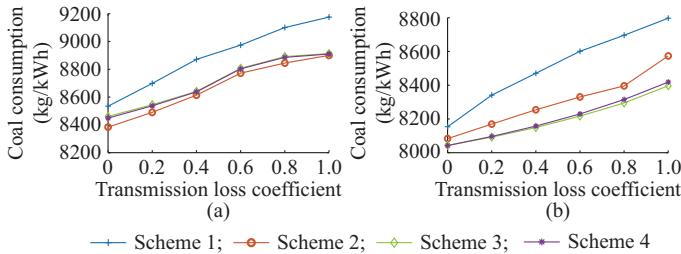


Fig. 10. Comparison of coal consumptions in four schemes. (a) $k_{down} = 0$ and $k_{up} = 0$. (b) $k_{down} = 0.25$ and $k_{up} = 0.25$.

The main difference between schemes 2 and 3 is that EBs are equipped in PHSN and SHSN, respectively. The heat outputs of CHP plants, EBs, and heat load in schemes 2 and 3 are presented in Fig. 11(a)-(c) when the heat load elasticity and heat loss are both zero, which is defined as case 1. Figure 11(d)-(f) presents the heat outputs and heat load when both the elasticity coefficients of heat load are 0.25, and the heat loss coefficient is 1.0, which is defined as case 2. Similarly, Fig. 12 presents the power outputs of TP plants, CHP plants, EBs, and wind power in the same simulation cases.

The coal consumption cost of the two modes is directly related to the utilization of the EBs. Furthermore, the utilization is mainly affected by the heat load elasticity and heat transmission. As the heat transmission efficiency decreases, the heat power transferred by the EBs equipped in PHSN and CHP plants will be partly lost in the transmission process. To compensate for the heat loss, CHP plants have to increase its heat output, which causes an increase in operation cost. The influence of heat load elasticity on operation cost can be analyzed through the comparison between cases 1 and 2. When the heat load is fixed, the operation constraint for the EBs in SHSN is stricter than those in PHSN. This is because the EBs in PHSN can provide heat to multiple heating areas, while the EBs in SHSN has to follow the heat load curve of its own heating area separately. Figure 11(b) presents that the heat output of the EBs in scheme 2 is higher than that of scheme 3. Therefore, both the heat output of CHP in Fig. 11(a) and power output in Fig. 12(b) decrease. The outputs of TP plants increase slightly with the premise that the wind power is completely consumed, which is shown in Fig. 12(a)-(d). Figure 11(e) shows that as the heat load elasticity increases, the fluctuation of the heat load is compensated preferentially by the EBs in SHSN, and its utilization significantly increases. For CHP plants shown in Fig. 11(d) and Fig. 12(f), the heat and power outputs of CHP are both reduced. The outputs of TP plants and wind power increase correspondingly, which indicates that the choice of these two schemes depends on the heat performance of the system.

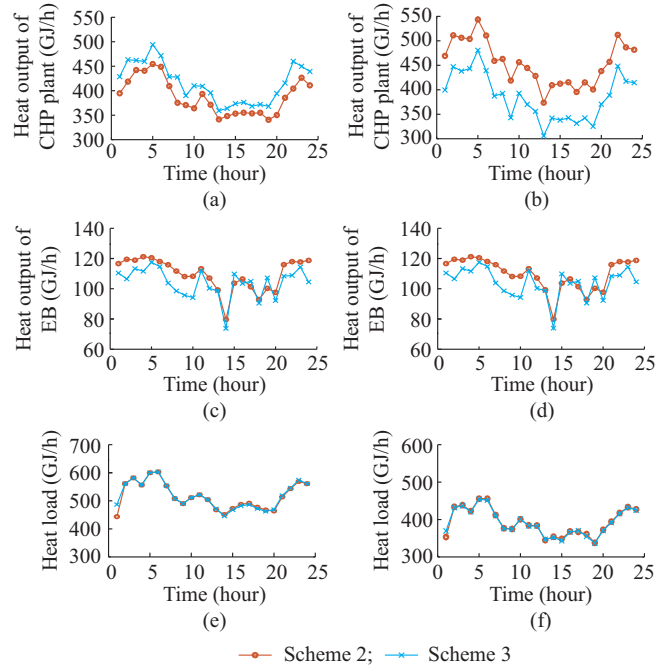


Fig. 11. Heat outputs of CHP plant, EBs, and heat load in schemes 2 and 3. (a) Heat output of CHP plant in case 1. (b) Heat output of CHP plant in case 2. (c) Heat output of EB in case 1. (d) Heat output of EB in case 2. (e) Heat load in case 1. (f) Heat load in case 2.

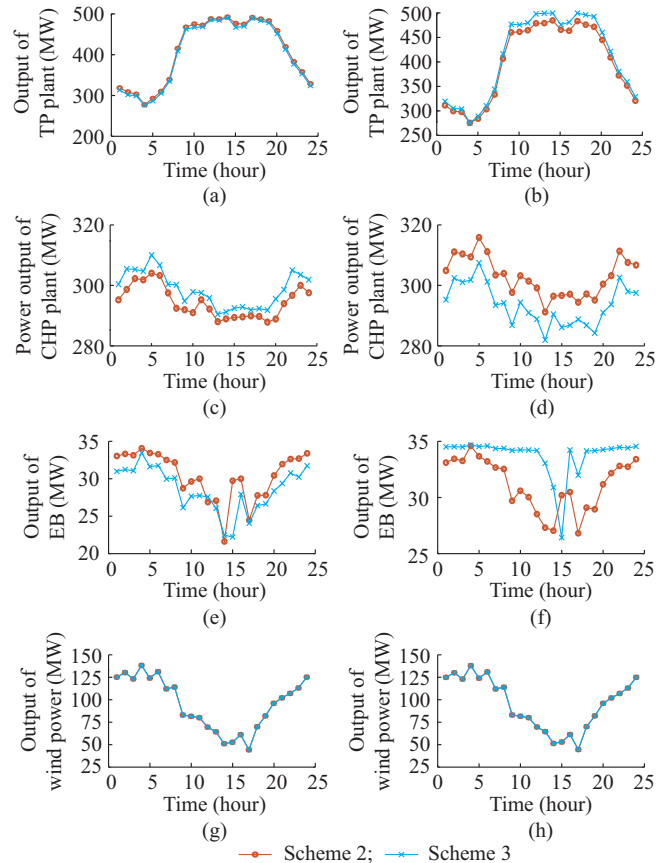


Fig. 12. Power outputs of TP plant, CHP plant, EB, and wind power in schemes 2 and 3. (a) Output of TP plant in case 1. (b) Output of TP plant in case 2. (c) Power output of CHP plant in case 1. (d) Power output of CHP plant in case 2. (e) Output of EB in case 1. (f) Output of EB in case 2. (g) Output of wind power in case 1. (h) Output of wind power in case 2.

II. CONCLUSION

We address the issue of wind power accommodation with CHP plants and EBs at different locations. The conclusions are given as follows.

1) The allocation of EBs is able to accommodate curtailed wind power. With no loss of heat-supply network, all the three schemes equipped with EBs succeed to achieve the accommodation of wind power curtailment. The curtailed wind power declines as the transmission efficiency of heat-supply network increases.

2) Coal consumptions in four schemes with no EBs, EBs only in PHSN, EBs only in SHSN, and EBs in both PHSN and SHSN all decrease with the enhancement of transmission efficiency of heat-supply network and the elasticity of heat load. And these two factors have different influences on the utility of the EBs at different locations. With the decrease of elasticity coefficient and the increase of heat transmission efficiency, the advantage of EBs in PHSN becomes more and more prominent. Similarly, with the increase of elasticity coefficient and the decrease of heat transmission efficiency, the utilization of EBs in SHSN will be more than that in PHSN.

3) Curtailed wind power absorbed by EBs is converted into heat energy to supply heat, which results in the reduction of heat output for CHPs. Hence, with the connection of EBs, the total power outputs of CHPs decline, trending with the variation of heat load.

4) The elasticity of heat load is not specific enough and the flexibility of heat demand may be more complex during the actual operation process, which can be further studied in the future. More constraints of the heat network such as the transmission capacity limitation will be considered further.

REFERENCES

- [1] National Bureau of Statistics. (2019. Jan.). National data. [Online]. Available: <http://data.stats.gov.cn/easyquery.htm?cn=C01>
- [2] Inner Mongolia People's Government. (2017. Apr.). "Thirteenth Five-Year" industrial development plan of inner Mongolia Autonomous Region. [Online]. Available: http://www.elht.gov.cn/tzcl/zsyz/yhzc/201808/t20180824_157547.html
- [3] R. Amirante, E. Cassone, E. Distaso *et al.*, "Overview on recent developments in energy storage: mechanical, electrochemical and hydrogen technologies," *Energy Conversion and Management*, vol. 132, no. 15, pp. 372-387, Jan. 2017.
- [4] F. Geth, T. Brijis, J. Kathan *et al.*, "An overview of large-scale stationary electricity storage plants in Europe: current status and new developments," *Renewable and Sustainable Energy Reviews*, vol. 52, pp. 1212-1227, Dec. 2015.
- [5] X. Luo, J. Wang, M. Dooner *et al.*, "Overview of current development in electrical energy storage technologies and the application potential in power system operation," *Applied Energy*, vol. 137, no. 1, pp. 511-536, Jan. 2015.
- [6] F. Geth, T. Brijis, J. Kathan *et al.*, "A review of energy storage technologies for wind power applications," *Renewable and Sustainable Energy Reviews*, vol. 16, no. 4, pp. 2154-2171, Dec. 2012.
- [7] B. Zakeri and S. Syri, "Electrical energy storage systems: a comparative life cycle cost analysis," *Renewable and Sustainable Energy Reviews*, vol. 42, pp. 569-596, Feb. 2015.
- [8] S. Sichilalu, T. Mathaba, and X. Xia, "Optimal control of a wind-PV-hybrid powered heat pump water heater," *Applied Energy*, vol. 185, pp. 1173-1184, Jan. 2017.
- [9] S. J. G. Cooper, G. P. Hammond, M. C. Mcmanus *et al.*, "Detailed simulation of electrical demands due to nationwide adoption of heat pumps, taking account of renewable generation and mitigation," *IET Renewable Power Generation*, vol. 10, no. 3, pp. 380-387, Mar. 2016.
- [10] P. Mancarella, "Cogeneration systems with electric heat pumps: energy-shifting properties and equivalent plant modelling," *Energy Conversion and Management*, vol. 50, no. 8, pp. 1991-1999, Aug. 2009.
- [11] S. Sichilalu, T. Mathaba, and X. Xia, "Optimal control of a wind-PV-hybrid powered heat pump water heater," *Applied Energy*, vol. 185, pp. 1173-1184, Jan. 2017.
- [12] T. S. Pedersen, P. Andersen, K. M. Nielsen *et al.*, "Using heat pump energy storages in the power grid," in *Proceedings of 2011 IEEE International Conference on Control Applications (CCA)*, Denver, USA, Sept. 2011, pp. 1106-1111.
- [13] J. Deng, L. Hu, and J. Li, "Analysis on mechanism of curtailed wind power accommodation and its economic operation based on electric boiler for peak-load regulation at secondary heat supply network," *Automation of Electric Power Systems*, vol. 40, no. 18, pp. 41-46, Sept. 2016.
- [14] X. Chen, C. Kang, and M. O. Malley, "Increasing the flexibility of combined heat and power for wind power integration in China: modeling and implications," *IEEE Transactions on Power Systems*, vol. 30, no. 4, pp. 1848-1857, Jul. 2015.
- [15] P. Meibom, J. Kiviluoma, and R. Barth, "Value of electric heat boilers and heat pumps for wind power integration," *Wind Energy*, vol. 10, no. 4, pp. 321-337, Jul. 2007.
- [16] M. B. Blarke, "Towards an intermittency-friendly energy system: comparing electric boilers and heat pumps in distributed cogeneration," *Applied Energy*, vol. 91, no. 1, pp. 345-365, Mar. 2012.
- [17] N. Zhang, X. Lu, and M. B. Mcelroy, "Reducing curtailment of wind electricity in China by employing electric boilers for heat and pumped hydro for energy storage," *Applied Energy*, vol. 184, no. 15, pp. 987-994, Dec. 2016.
- [18] X. Jiang, Z. Jing, Q. H. Wu *et al.*, "Modeling of a central heating electric boiler integrated with a stand-alone wind generator," in *Proceedings of 2013 IEEE PES Asia-Pacific Power and Energy Engineering Conference (APPEEC)*, Hong Kong, China, Dec. 2013, pp. 1-6.
- [19] M. G. Nielsen, J. M. Morales, and M. Zugno, "Economic valuation of heat pumps and electric boilers in the Danish energy system," *Applied Energy*, vol. 167, no. 1, pp. 189-200, Apr. 2016.
- [20] S. Rong, Z. Li, and W. Li, "Investigation of the promotion of wind power consumption using the thermal-electric decoupling techniques," *Energies*, vol. 8, no. 8, pp. 8613-8629, Aug. 2015.
- [21] J. Li and L. Hu, "Research on accommodation scheme of curtailed wind power based on peak-shaving electric boiler in secondary heat supply network," *Power System Technology*, vol. 39, no. 11, pp. 3286-3291, Nov. 2015.
- [22] Z. Gu, C. Kang, and X. Chen, "Optimization of integrated power and heat energy systems and the benefit on wind power accommodation considering heating network constraints," *Proceedings of the CSEE*, vol. 35, no. 14, pp. 3596-3603, Jul. 2015.
- [23] Z. Li, W. Wu, M. Shahidehpour *et al.*, "Combined heat and power dispatch considering pipeline energy storage of district heating network," *IEEE Transactions on Sustainable Energy*, vol. 7, no. 1, pp. 12-22, Jan. 2016.
- [24] C. Wu, W. Gu, P. Jiang *et al.*, "Combined economic dispatch considering the time-delay of district heating network and multi-regional indoor temperature control," *IEEE Transactions on Sustainable Energy*, vol. 9, no. 1, pp. 118-127, Jan. 2018.
- [25] L. Lin, J. Gu, and L. Wang, "Optimal dispatching of combined heat-power system considering characteristics of thermal network and thermal comfort elasticity for wind power accommodation," *Power System Technology*, vol. 43, no. 10, pp. 3648-3655, Oct. 2019.
- [26] J. Li and L. Hu, "Research on accommodation scheme of curtailed wind power based on peak-shaving electric boiler in secondary heat supply network," *Power System Technology*, vol. 39, no. 11, pp. 3286-3291, Nov. 2015.
- [27] B. Stott, J. Jardim, and O. Alsac, "DC power flow revisited," *IEEE Transactions on Power Systems*, vol. 24, no. 3, pp. 1290-1300, Aug. 2009.
- [28] B. Liu and K. Iwamura, "Chance constrained programming with fuzzy parameters," *Fuzzy Sets and Systems*, vol. 94, no. 2, pp. 227-237, Mar. 1998.
- [29] H. V. Larsen, B. Bohm, and M. Wigbels, "A comparison of aggregated models for simulation and operational optimisation of district heating networks," *Energy Conversion and Management*, vol. 45, no. 7, pp. 1119-1139, May 2004.
- [30] S. Yuan, "Research on dynamic performance of centralized Heat-supply System," M. S. thesis, Environment College, Tianjin University, Tianjin, China, 2010.

Yunfeng Ma received the B.S. degree in electrical engineering in 2017 from North China Electric Power University, Baoding, China. She is currently pursuing the Ph.D. degree at the School of Electrical and Electronic Engineering, North China Electric Power University, Beijing, China. Her research interests include optimal dispatching and control of thermostatically controlled load.

Yang Yu received the M.S. degree in electrical engineering from Xi'an Jiaotong University, Xi'an, China, in 2008, and the Ph.D. degree in electrical engineering in 2016 from North China Electric Power University, Beijing,

China. He is currently an Associate Professor at North China Electric Power University, Baoding, China. His research interests include electrical energy storage technology, and optimal dispatching of flexible load.

Zengqiang Mi received the M.S. degree in electrical engineering from North China Electric Power University, Baoding, China, in 1986. He is currently a Professor at North China Electric Power University, Beijing, China. His research interests include power system operation and control, electrical energy storage technology, and optimal dispatching of flexible load.